Desalination and Water Treatment
www.deswater.com
doi: 10.5004/dwt.2023.29176

284 (2023) 39–48
February

Investigation of oily wastewater treatment by few-layer graphene adsorbent and UV-Vis spectral analysis

Hamid Motahari*, Parvaneh Haghighi, Mohsen Khajeh Aminian

Department of Physics, Yazd University, Yazd, Iran, emails: H.Motahari@Yazd.ac.ir ORCID No: https://orcid.org/0000-0001-5898-7731 (H. Motahari), parihaghighi114@gmail.com (P. Haghighi), kh.aminian@yazd.ac.ir (M.K. Aminian)

Received 22 July 2022; Accepted 27 November 2022

ABSTRACT

In this study, few-layer graphene (FLG) has been applied for oily wastewater treatment. Seven types of oils, including engine oil, olive oil, sesame oil, corn oil, castor oil, and two types of cooking edible oil, Oila and Aftab brands, have been examined. 0.1 g of a few-layer graphene adsorbent has been used. The results show that it can absorb 5 mL engine oil with 99% removal efficiency, castor oil to 98%, Oila and Aftab to 97%, olive oil to 96%, corn oil, and sesame oil to 93%. The adsorption capacity for these seven types with more than 95% removal efficiency is 25 to 43 g/g. The increasing oil/water ratio can cause decreasing removal efficiency for sesame oil, corn oil, Oila, and Aftab. Generally, it indicates that removal efficiency depends on oil type and oil/water ratio. Also, the FLG can remove real oils from oily wastewater at less than 120 s in a FLG filter column. Indeed FLG as a proper light absorbent can decrease the wastewater total dissolved solid from 520 to 25 ppm. Also, the hybrid of adsorption and light absorption ability of FLG can use effectively in wastewater treatment.

Keywords: Few-layer graphene; Oily wastewater; Removal efficiency; Adsorbent

1. Introduction

The water crisis and water shortage has become a significant problem in arid regions, such as Middle East [1]. It has been estimated that 70% of the world population will face water shortage issues by 2025 [2]. Indeed, water pollution as a dangerous threat to the ecosystem has become a growing concern [3]. Also, increasing water demand for human life, such as industrial and public uses, requires more water. One of the essential supply methods is water recycling or wastewater treatment. Generally, all water sources need a proper treatment process. On the other hand, rapid economic growth directly depends on global oil consumption. Oil is a raw material source for thousands of substances and also is the most indispensable energy source. Nowadays, 100 million tons of oil-based products produce in the world annually. Therefore, oil pollution has become one serious concern [4]. Oil pollution impact and environmental toxicity have been increased in the past few years [5]. Oil and its products can significantly pollute the waters of oceans, seas, and groundwater. Wherever oil and petroleum products are produced, transported, and stored, there is a risk of spillage and contamination of the environment. It has been estimated that between 2000 and 2011, about 224,000 tons of oil have been released into the marine environment. One of the main sources of water pollution is the crude oil spill. Oil spill over the oceans and seas requires prompt attention due to their environmental and economic impacts. Spilled oil has an undesirable odor and causes severe water pollution and environmental damages. The spilled oil eventually enters toxic components into the human food chains and affects our health. Therefore, spilled oil causes enormous environmental problems unless removed as quickly as possible [6]. Therefore, one of the most essential environmental issues is oily wastewater, especially in the Middle East region due to large oil fields and crude oil resources

* Corresponding author.

[7]. The oily wastewater pollution affects groundwater resources, oceans, and soil. Oily wastewater pollution affects crop production and human health via drinking water [8]. Therefore, oily wastewater treatment techniques are so important issues, especially for oil processing companies, petrochemical companies, pharmaceutical, and food industries [9]. These industries are the most productive source of oily wastewater. Moreover, oil tanker or petroleum tanker always has the risk of an oil spill because these tankers have been designed for bulk transport of crude oil or its product on the oceans. However, oil-rich countries and all other countries encounter oily wastewater treatment every day. Also, the removal of spilled oil into the water structure has become a global problem. The other challenge is time that is almost so important factor. In the last years, more attention has been focused on the treatment techniques for oily wastewater [9]. These problems must be explored and resolved by researchers by low-cost, and high efficient approaches [2]. The main methods for controlling oil leakage are oil adsorbents, *in-situ* combustions, chemical flocculants, and microbiological degradation. Oil adsorbent is the most effective and efficient method on a large scale. Generally, other techniques have some side effects and disadvantages, such as wasting large amounts of resources at the *in-situ* combustion method, long process time at the microbiological degradation method, and secondary pollution in the chemical dispersions method [10]. It is possible to open new paths for oily wastewater treatment with the technology innovation and new adsorbent materials such as graphene, few-layer graphene (FLG), and multi-layer graphene, new carbon nanostructures, etc. [11–13]. One of the efficient methods for the removal and absorption of oil pollutants is carbon nanostructures while the water adsorption will not occur. The exotic physical properties of graphene and graphene oxide have led to intense research activities [14–16]. The new generation of materials such as few-layer graphene and exfoliated graphite are good choices, especially for oily wastewater treatment. Therefore, many researchers have been worked on water treatment, and oily wastewater by FLG, and graphene based materials [17–22]. For example, a cellulose-based oil adsorbent has been developed, and the capability of the product to absorb engine oil, kerosene, and xylene has been studied. This adsorbent had an excellent performance with high absorbing ability of 16–28 times its weight [10]. In the present work, few-layer graphene (FLG) has been synthesized, and used as oil adsorbent material. The quality and quantity of oil adsorption process by FLG are significant factors for oily wastewater treatment. Some research aspects of FLG adsorbent, such as removal efficiency, adsorption ability, and oil adsorption capacity for various types of oils, should be investigate by this oil adsorbent candidate. Indeed, the FLG capability as hybrid wastewater treatment tool can investigate as adsorbent of oil pollution from water and light absorption in water evaporation purification method.

2. Materials and methods

In this study, FLG has been synthesized by chemical exfoliation of graphite flakes in microwave oven, and then it has been used as the adsorbent. Several oils, including engine oil, olive oil, sesame oil, corn oil, castor oil, and two types of cooking edible oil, Oila and Aftab brands, have been used as water pollutants. These seven types of oil have been shown in Fig. 1. The density of oil pollutants according to the relation $\rho = m$ (g)/V (cm^3) has been reported in Table 1.

This study evaluates the removal of some oil pollutants from water using few-layer graphene and residual exfoliated

Table 1
Density of oils that have been used as water pollutants in this research

Oil pollutant	m (g)	V (cm^3)	ρ (g/cm^3)
Engine oil	4.378		0.875
Olive oil	4.631		0.926
Sesame oil	4.403		0.880
Corn oil	4.721	5	0.944
Oila	4.741		0.948
Castor oil	4.339		0.867
Aftab	4.494		0.898

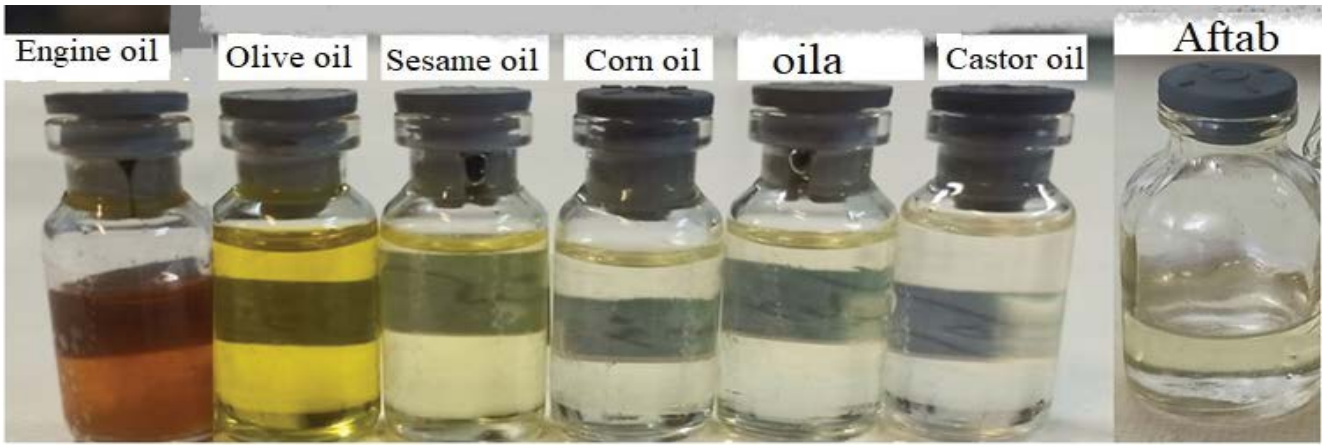

Fig. 1. Seven types of oils as pollutants in oily wastewater have different colors.

graphite. The characterization methods such as micro-Raman and Fourier-transform infrared spectroscopy (FTIR), field-emission scanning electron microscopy (FESEM), X-ray diffraction (XRD), energy-dispersive X-ray spectroscopy (EDX), and Brunauer–Emmett–Teller (BET) analysis have been applied for evaluating the fabricated FLG. Also, UV-Vis spectroscopy has been used for oils characterization and oil adsorption ability.

The morphological properties of FLG have been characterized using the scanning electron microscope (SEM), Tescan VEGA3 model, and FESEM, Tescan Mira 3 model. Raman spectroscopy is one of the best methods to characterize various types of multi-layer graphene, few-layer graphene, and finally, single-layer graphene compared to graphite [23,24]. The FLG properties have been investigated by TakRam N1-541 laser micro-Raman spectroscopy using Nd:YAG laser in its second harmonic generation at 532 nm wavelength. FTIR has been applied using the Bruker, EQUINOX55 by mixing KBr in the tablet shape. FTIR spectroscopy can detect the vibrational modes of the structure. XRD analysis from graphite powder and FLG powder has been done by the Bruker D8 ADVANCE model and Cu anode with 1.54 Å as X-ray wavelength. The BET has been taken by BELSORP MINI II model for determination of surface area and pore size analysis. In the experimental section, seven types of oily wastewater have been fabricated in our laboratory. The oily wastewater treatment test is performed by mixing 1, 3, 5 mL oil, and 20 mL of water. Oils as contaminants are poured into a cylinder with the ratios 1:20, 3:20, and 5:20 of oil:water. These emulsions have been mixed with a magnetic stirrer and ultrasonic bath thoroughly. After that, removals of oils by adding 0.1 g FLG powder to oil-water emulsion have been investigated. The FLG adsorbent powder has been added to oils/water emulsion. After 10 min, it has been filtered using a sieve. The volumes of water and oil contaminant mixture have been recorded before separation. For example, Oila and engine oil on the water can be seen in Fig. 2a and b, respectively. The next step is adding 0.1 g FLG to the emulsion, as shown in the middle columns in Fig. 2a and b. In the final stage, the oily FLG as a black bulk material has been removed by a 325 stainless steel mesh sieve. Therefore, transparent residual water has shown in the third columns of Fig. 2a and b. FLG and oil contaminant as a bulk mass can be seen in Fig. 2c, and it has been separated easily.

Finally, two methods, including pads and cylindrical tubes, have been used in this research to find the better FLG adsorbent separation route from residual water. The pad had a 1.5 cm × 3 cm rectangular shape from polypropylene, as schematically shown in Fig. 3a. In the other separation method, the FLG cylindrical tube filter has been shown in Fig. 3b. Its dimension was about 1 cm in diameter and 25 cm in height. Fig. 3c shows a schematic design for oil adsorption on FLG. Both methods had similar results without significant differences in the adsorption capacity but the cylindrical tube is faster in time. The adsorption ability of studied oils depends on the physical bonds between FLG and surface groups of oil molecules as shown in Fig. 3c. The polar strength of oil chemical groups and number of these surface groups in the molecule are high effective in the oil adsorption ability. Also the adsorption ability of oils could be depended on the length of molecule chain. The longer chain molecule can make more physical bonds on the surface of FLG and results in higher adsorption ability. Also, the oil removal from water is due to its lipophilic and hydrophobic properties, so the FLG cannot absorb water from the oily wastewater.

3. Results and discussion

3.1. FLG characterization

The scanning electron microscope (SEM) and FESEM characterization results of exfoliated graphite and few-layer graphene can be seen in Fig. 4a–d, respectively. The powders sample has a stacked layer structure, such as few-layer and multi-layer graphene. The single layer or few-layer graphene is so hard to detect directly by FESEM or SEM analysis. Therefore, the exfoliated graphite before expanding has been analyzed. However, it seems the average thickness of layers is less than 20 nm in exfoliated graphite.

Table 2 shows the EDX quantitative result of FLG. It shows the atomic percent of the FLG is about 96% carbon

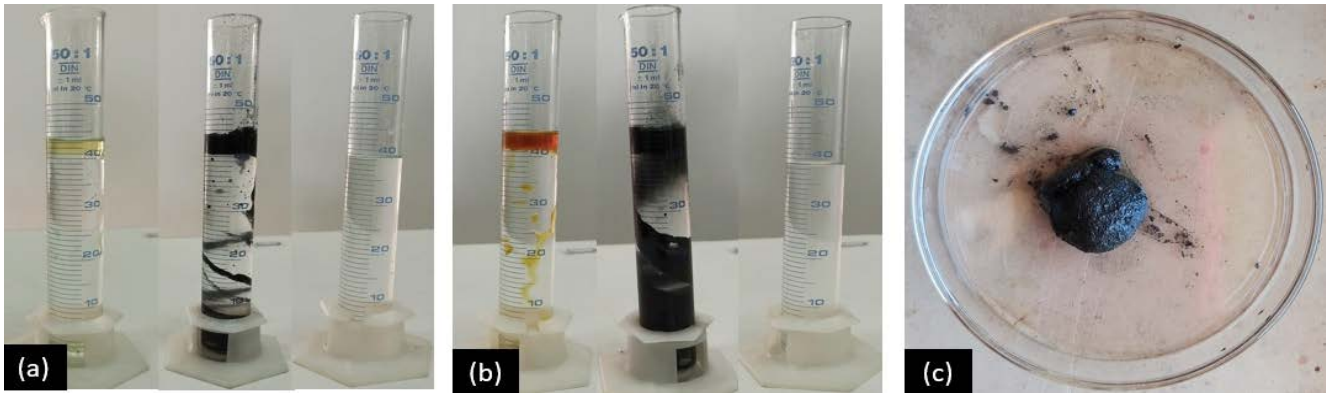

Fig. 2. The left hand pictures correspond to Oila and engine oil in water in (a) and (b), respectively. The next step is adding 0.1 g FLG to the emulsion, as shown in middle columns. In the final stage that separation has occurred, transparent residual water has shown in the third columns. (c) The FLG and oil contaminant as a bulk mass can be seen, and it has been separated easily.

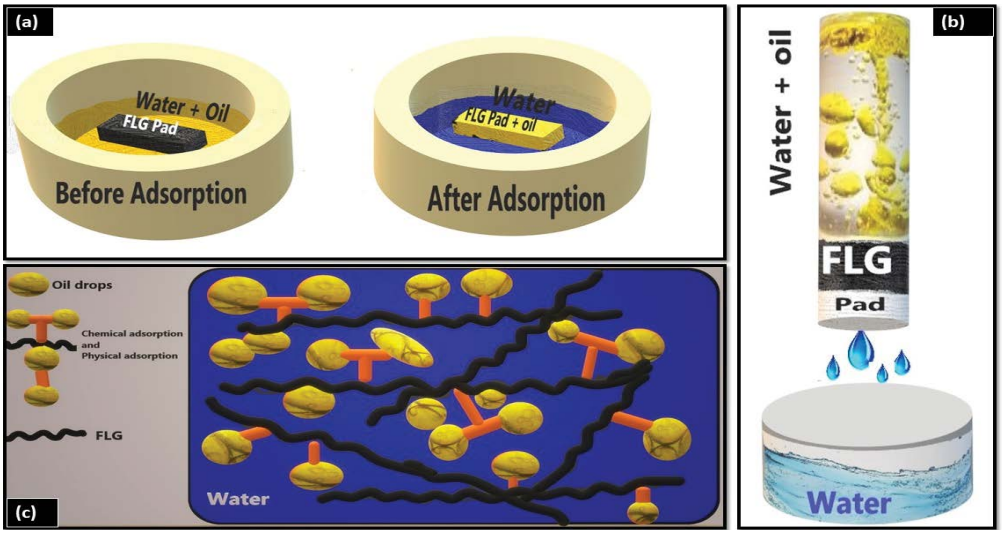

Fig. 3. Schematic diagram of (a) FLG pad, (b) cylindrical tube filter of FLG, and (c) oil removal process by FLG from water.

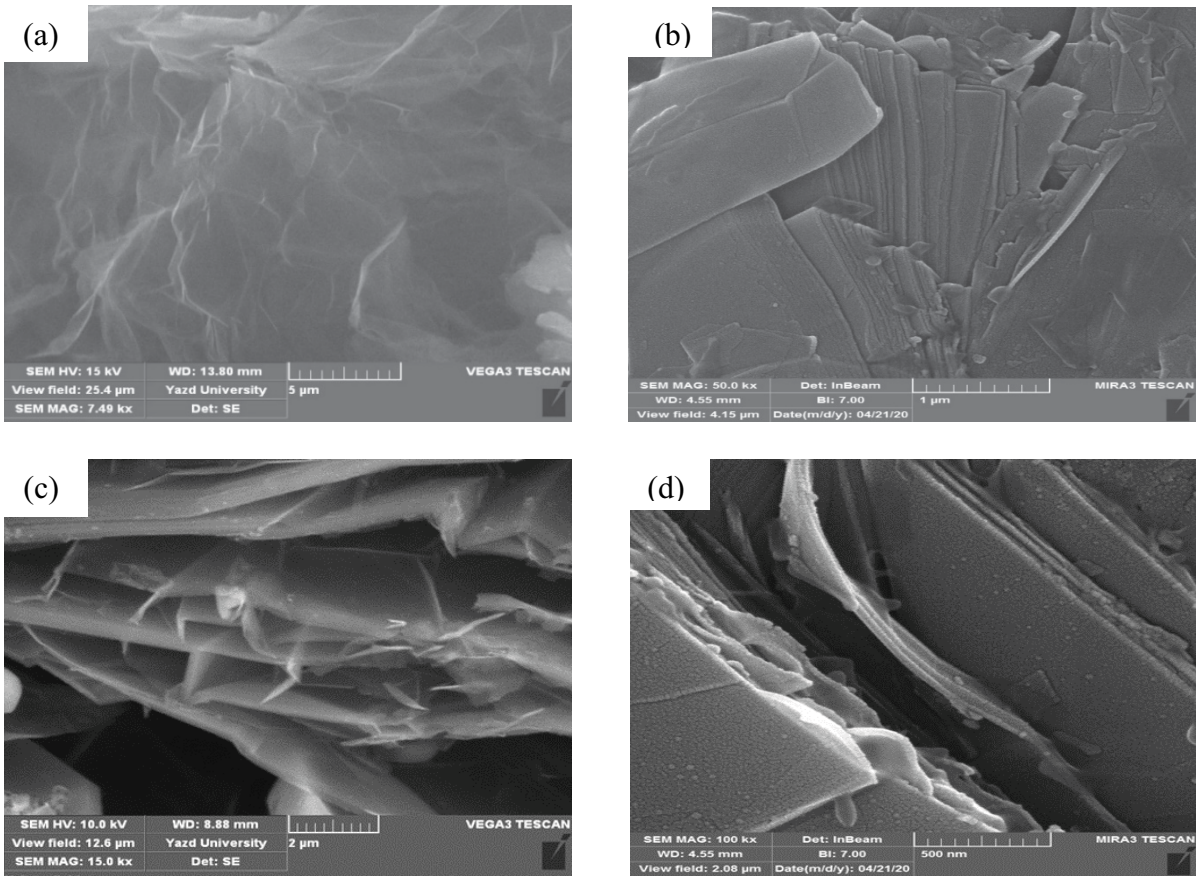

Fig. 4. SEM and FESEM images of (a, b) exfoliated graphite and (c, d) FLG.

and there is 3.63% oxygen in the sample due to oxygen adsorb on the surface or even graphene oxide phase in the samples.

Fig. 5 indicates the micro-Raman spectra of FLG powder. The I_{2D}/I_G peak intensity ratio is about 0.6, and the disordered band (D-band) is weak.

Also, the graphitic band (G-band) has a sharp peak at around 1,570 cm^{-1} in the Raman shift position. The main features in the Raman spectrum of graphite-based carbon structures are the presence of G and D bands and the second-order or 2D peak. The position, relative intensity, displacement of the peak location, and FWHM of these three bands

can be different in carbon-based materials. The G-band or graphitic band at around 1,580 cm^{-1} corresponds to the tensile vibrations of carbon atoms in a plane [25]. In other words, the presence of this band with high intensity indicates regular graphite plates and regular single crystal graphite crystal lattice. Therefore this band becomes more intense by increasing the number of carbon atoms in different layers that contribute to the vibration state. However, its severity, shape, and position are sensitive to any intentional and unwanted impurities. The position and presence of the D-band or disordered band indicate the presence of crystal defects in the arrangement of atoms in the structure of graphite honeycomb networks. The weak signal of the D-band shows that the graphitic structure has no defects or even impurities. However, the intensity and appearance of the D band also depend on the laser excitation energy. Also, the D band is the respiratory mode due to the hexagonal loops, and I_D/I_G indicates the number of loops at the edge of the grain.

Table 2
EDX quantitative results of FLG

Elt	W%	A%
C	94.15	95.91
O	4.74	3.63
Na	0.45	0.24
S	0.25	0.10
Cl	0.16	0.06
Ca	0.25	0.07
	100	100

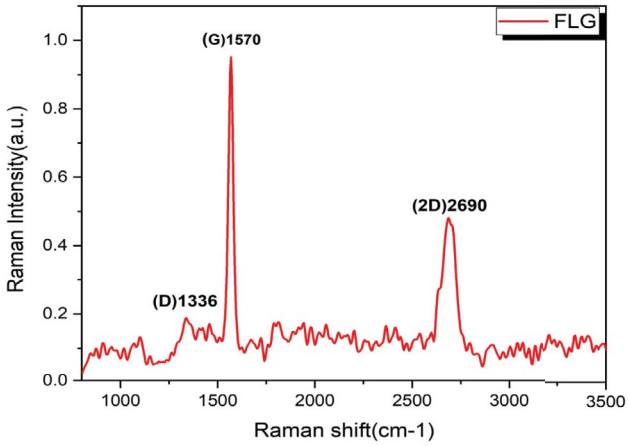

Fig. 5. Micro-Raman spectra of FLG.

The intensity of the D band decreases due to a decrease in the number of loops in the clusters. However, the 2D band as a second vibrational mode of the D band occurs around 2,700 cm^{-1}. Sometimes, the presence of the 2D band is one of the main signs of graphene structure, and it is the significant difference between graphite and graphene. Therefore, the type of graphene is almost few-layer and multi-layer graphene [26]. Also, the micro-Raman method evaluation predicts that the average of layers is about six layers [27]. Fig. 6 shows the XRD of few-layer graphene in comparison with graphite. This pattern indicates that the crystalline structure of FLG and graphite are the same because of the same peak positions at about 26.54° and 44.5° for 2θ [26,28]. The *d*-space is about 3.355 and 2.03 Å, respectively. The intensity ratio of FLG to graphite powder is about 0.05. The layer number of FLG is so little in comparison with graphite powder.

The surface area measurement of a powder is an essential factor that determines the porosity of nanomaterials. BET is a technique that is generally used to determine the porosity and surface area of microporous and mesoporous materials. Microporous and mesoporous materials have some features, such as pore-size distribution and the volume of pores [29]. The adsorption–desorption diagram for FLG has been shown in Fig. 7a. The result of the BET measurement for the FLG sample shows that the surface area is 9.35 m^2/g. The Barrett–Joyner–Halenda (BJH) plot of FLG shows the pore-size distribution of the sample in Fig. 7b. The average pore size of this sample is measured 17.2 nm.

FTIR spectroscopy can give the molecular tendency to attach to an adsorbent surface. FTIR characterization of graphite and FLG has been shown in Fig. 8. There are some small differences between them as shown in the figure.

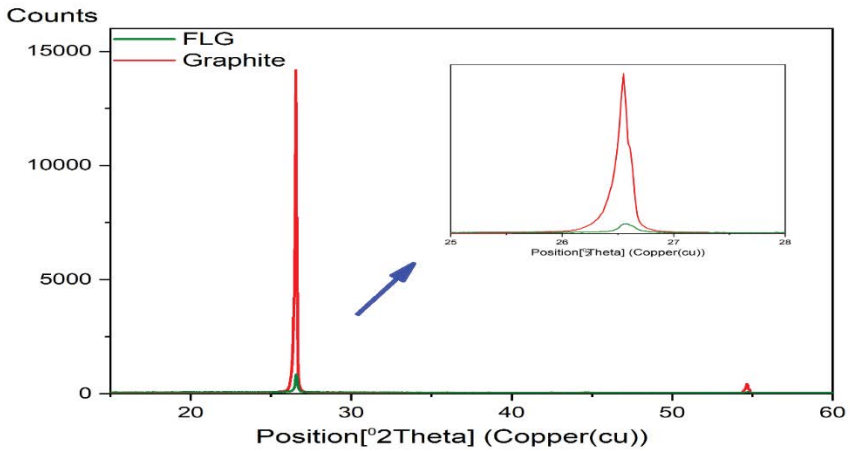

Fig. 6. XRD of graphite and FLG.

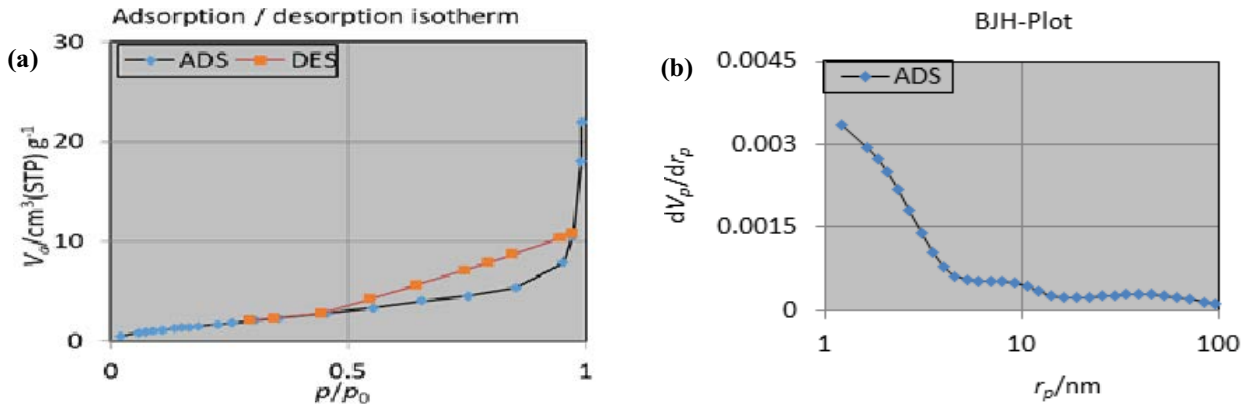

Fig. 7. (a) The adsorption–desorption diagram and (b) BJH – plot; the pore-size distribution of FLG sample.

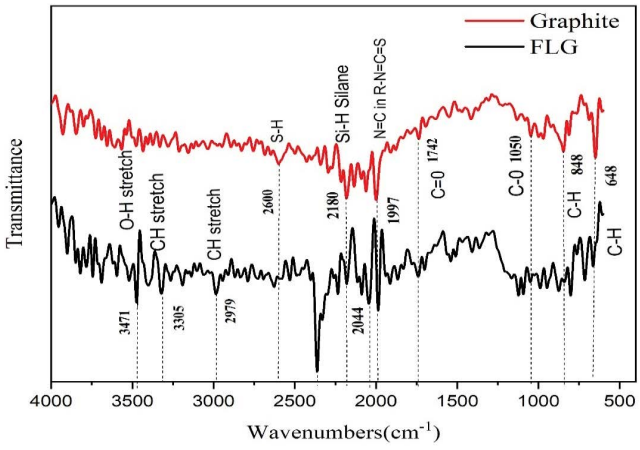

Fig. 8. FTIR diagram for FLG and graphite.

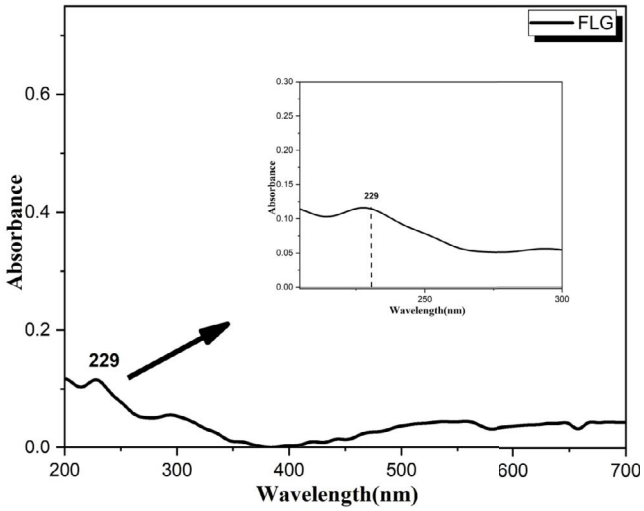

Fig. 9. UV-Vis spectrum of FLG suspension in distilled water shows a broadband peak at 229 nm.

In addition, the UV absorption FLG peak is a broad band peak at about 228–230 nm, as shown in Fig. 9. This peak is corresponding to $\pi \rightarrow \pi^*$ transitions for the C double bonds bonding. Also, the peak around 270–300 nm is attributed to the $n \rightarrow \pi^*$ transition of the carbonyl groups (C double bond O) [30].

3.2. Oil characterization by UV-Vis spectroscopy

UV-Vis spectroscopy is the characterization method for oil analysis and the aqueous solution is entirely transparent in this region. The linear relationship between optical absorbance, A (or optical density, OD), and concentration has been developed and called Beer–Lambert law equation. The oil characterization by UV-Vis spectroscopy is a proper and fast method [31,32]. For example, olive oil has many fatty acids, such as stearic, linolenic, palmitic, oleic, and linoleic. The UV-Vis is a helpful tool to detect the presence of virgin olive oil in the olive oil. Virgin olive oils show emission at 673 nm due to the presence of chlorophyll, and it is different from refined olive oil [33]. Lubricating oils are the most valuable constituents of crude oil. Used lubricating oils are by-products of oil used in vehicles and machinery. They must be replaced regularly in all operating equipment

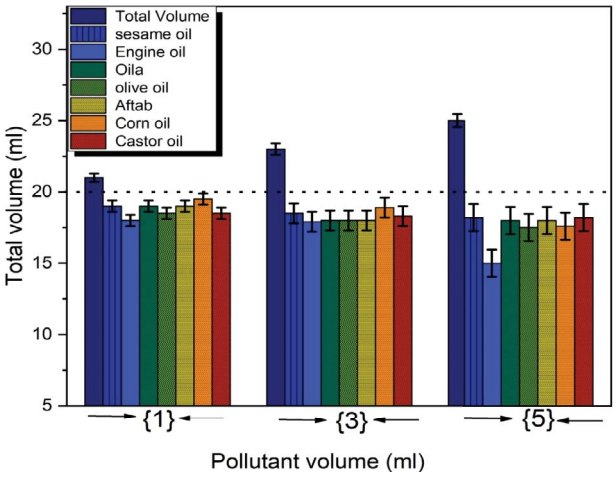

Fig. 10. One, three, and five milliliters (mL) oil as a pollutant in 20 mL water. The first column is total emulsion volume, and the other columns are related to the oil removed samples by 0.1 g FLG. The comparison shows that the FLG can effectively remove oils from emulsion.

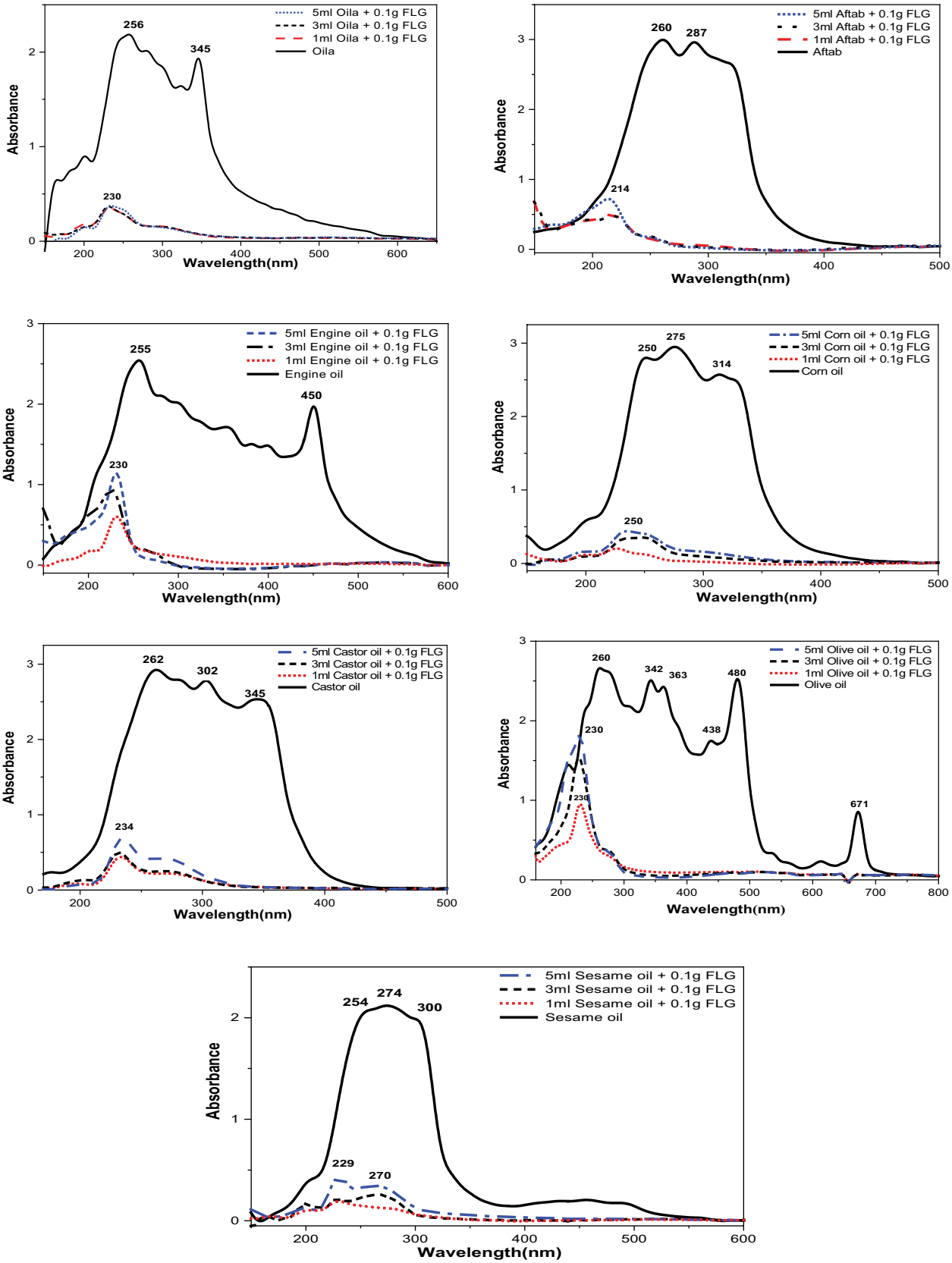

Fig. 11. The UV-Vis spectra are related to Oila, Aftab, engine oil, corn oil, castor oil, olive oil, and sesame oil in black color. Adding 0.1 g FLG to mixtures of 1, 3, and 5 mL oil and 20 mL water has been done. The sieving of suspension and UV-Vis spectrums has been shown in dash lines.

due to the contamination of dirt, water, salt, metals, incomplete products of combustion, or other materials [34]. Also, the other group of oils is edible oils such as sesame oil and olive oil. Sesame oil is the oldest oil seeds known to man, and many factories produce several hundreds of cubic meters of oily wastewater per day around the world. Their effluent is so oily wastewater, and they have many problems for the environment.

3.3. Oily wastewater treatment by FLG

The volumes of water and oil contaminant mixture have been recorded before FLG adsorbent separation. Then the volume of the emulsion after sieving has been recorded, as shown in Fig. 10 for comparison purposes. The figure shows three volumes of oil as pollutants in water in the range of 1, 3, and 5 mL. The first column is total emulsion volume, and the other columns are results after oil removal by 0.1 g FLG.

The comparison shows that the FLG can effectively remove oils from emulsions. The residual water in the three oil ranges is approximately constant. Also, it seems that the higher amount of oil pollutant in the emulsion can cause a small amount of water to be separated in water from the water-oil mixture due to water trapped between the adsorbed oil droplets on FLG. After that, UV-Vis spectroscopy in the range of 200–1,100 nm has been taken. Also, the oil concentration in water after the removal process can be extracted based on the optical absorbance of UV-Vis spectra. The results have been extracted using the maximum peaks in the spectra, as shown in Fig. 11. Indeed, the following equation is used for the definition of oil removal efficiency [6]:

$$\text{Removal Efficiency}(\%) = \frac{(C_0 - C_e)}{C_0} \times 100 = \frac{(A_0 - A_e)}{A_0} \times 100 \quad (1)$$

The spectrums show high-efficiency oil adsorption up to a maximum of 99% removal efficiency. Fig. 12 shows the efficiency of three samples, 1, 3, and 5 mL of oil volume in a plot. It can be observed that the oil adsorptions ability and efficiency depend on the type and composition of the oil. The increasing oils contamination in water can cause decreasing removal efficiency for sesame oil, corn oil, Oila, and Aftab, while there are no changes for engine oil, castor oil, and olive oil. The results show that the 0.1 g of FLG can absorb 5 mL engine oil with about 99% removal efficiency, castor oil to 98%, Oila and Aftab to 97%, olive oil to 96%, corn oil, and sesame oil to 93%. The adsorption capacity for these seven types of oils is between 25 to 28 g/g, with a removal efficiency of more than 95%. Generally, the adsorption oil capacity of FLG is at least 43 g/g with more than 93% removal efficiency. The best efficiency is for 1, 3, and 5 mL, respectively. Therefore, the high removal efficiency in oil adsorption up to about 99%, the short time, and very fast adsorption in less than 10 min are good results. In addition, the high capacity from about 25 g/g to about 43 g/g oil adsorption for various types of oils indicates that the FLG is a proper candidate for various types and compositions of oils. On the other hand, the price of this graphene-based material is so lower price than the single-layer or two-layer graphene. In the final step, a sample of real oily wastewater from the Sesame Factory has been prepared due to the

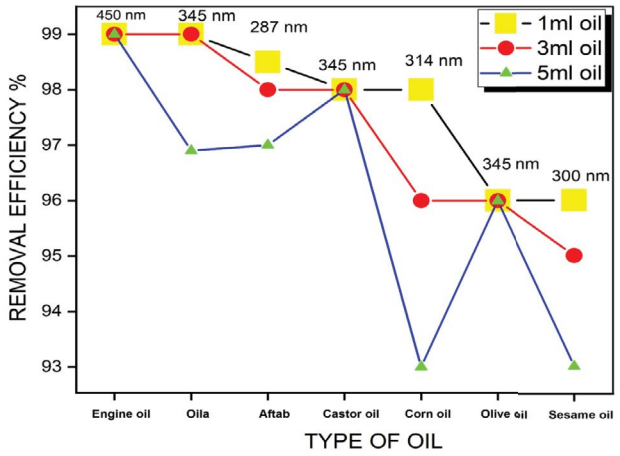

Fig. 12. Comparison removal efficiency of seven oil samples.

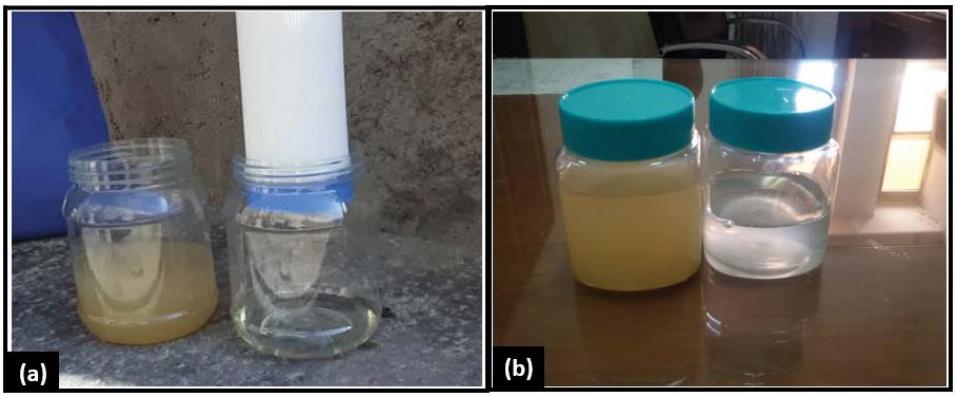

Fig. 13. (a) The photo shows the oily wastewater of the sesame oil production factory as a dirty yellowish color. After treatment by FLG filter column (white plastic with a blue cap), the permeate water is colorless oil-free in a bottle. (b) Sesame dirty yellowish color oily wastewater compares with colorless permeate water.

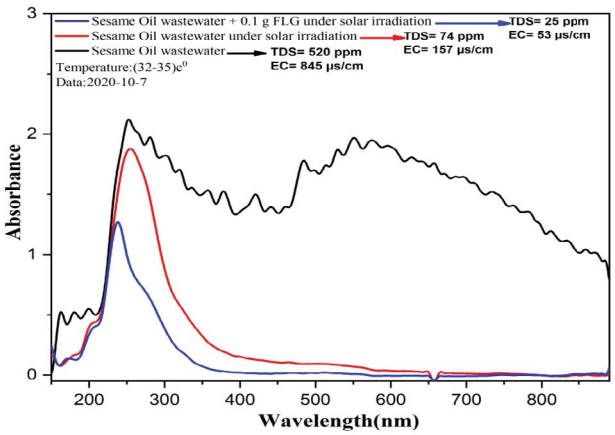

Fig. 14. The oily wastewater of Sesame Factory in Yazd under solar irradiation and FLG adsorption.

minimum removal efficiency of sesame oil. This oily wastewater fed vertically into the FLG filter tube. The tube with about 6 cm diameter and 15 cm height has been filled with FLG powder. Influent oily wastewater emulsion fed into it, and the effluent water immediately exits as transparent water without oil and color, as shown in Fig. 13.

3.4. Sesame oily wastewater purification by FLG adsorption and solar absorption capability of FLG

The real oily wastewater from the Sesame Factory has been prepared again. This sample had the minimum removal efficiency of sesame oil. Therefore, the combination water purification method has been applied. In this approach, two sesame oily wastewater samples have been prepared. The first one fills in the transparent PET dish with a door cap. The FLG powder has been covered on the top surface of wastewater in the second one. Both of them have been located under solar irradiation for 5 h a day in the same position in Yazd, Iran. Evaporated water results have been collected and analyzed, as shown in Fig. 14. The results show that FLG powder act as a good adsorbent from oily wastewater and a good light absorber for accelerating water evaporation. The second sample has been evaporated completely, about 45 min earlier than the first one. In the other word, the evaporation rate was about 15% more efficient by FLG in the environment temperature (32°C–35°C). Indeed, the total dissolved solid and EC decrease from 520 ppm and 845 µS/cm to about 25 ppm and 53 µS/cm. Therefore, it seems, FLG can be a good candidate for this hybrid water purification method.

4. Conclusions

Oily wastewater treatment by FLG has been evaluated for some types of edible and industrial oils. The oil removal from water is due to its lipophilic and hydrophobic properties, so the FLG cannot absorb water from the oily wastewater. FLG adsorbent powder has been used, and then UV-Vis spectra have been taken. The removal efficiencies were 93%–99% for seven types of oils in this research. The results show that the 0.1 g of FLG can absorb 5 mL engine oil with about 99% removal efficiency, castor oil to 98%, Oila, and Aftab to 97%, olive oil to 96%, corn oil, and sesame oil to 93%. The adsorption capacity for these seven types with more than 95% removal efficiency is between 25 to 43 g/g. Therefore the minimum adsorption capacity is about 25 g/g for seven types of oils in this research with more than 95% confidence interval removal efficiency. The increase of oil contamination in water up to 5 mL can cause decreasing removal efficiency for sesame oil, corn oil, Oila, and Aftab, while there are no changes for engine oil, castor oil, and olive oil. The FLG can remove various oils, but removal efficiency depends on oil type and oil/water ratio. It can be an efficient adsorbent that eliminates oil from oily wastewater in less than 120 s in a FLG filter column. In all seven samples, both quantity and quality for oil removal are essential. Moreover, it seems that, there is no relation between oil densities and removal efficiency. Therefore, both the quality and quantity of adsorption process by FLG are proper for oily wastewater treatment, especially as a pretreatment stage in water purification purposes. The oil adsorption ability to about 99% removal efficiency, and very fast adsorption in less than a few minutes, besides the good capacity from about 25 g/g to about 43 g/g for various types of oils, indicates that the FLG is a proper oil adsorbent candidate. Indeed FLG is a proper light absorbance, and it can use as hybrid wastewater treatment tool, adsorbent of oil pollution from water and light absorption for water evaporation purification method.

Acknowledgments

Financial support from the Yazd University is gratefully acknowledged.

Declarations

Funding

No funding was received for this study.

Conflicts of interest

The article does not face with any scientific or financial conflicts of interest.

Availability of data and material: not applicable

Code availability: Not applicable

Authors' contributions

H. Motahari: experiment, writing, editing and supervision; P. Haghighi: experiment and writing; M. Khajeh Aminian: editing and advisory.

References

[1] S. Gorjian, B. Ghobadian, Solar desalination: a sustainable solution to water crisis in Iran, Renewable Sustainable Energy Rev., 48 (2015) 571–584.
[2] C. Li, Y. Goswami, E. Stefanakos, Solar assisted sea water desalination: a review, Renewable Sustainable Energy Rev., 19 (2013) 136–163.

[3] B.Y.Z. Hiew, L.Y. Lee, X.J. Lee, S. Thangalazhy-Gopakumar, S. Gan, S.S. Lim, G.-T. Pan, T. Chung-Kuang Yang, W.S. Chiu, P.S. Khiew, Review on synthesis of 3D graphene-based configurations and their adsorption performance for hazardous water pollutants, Process Saf. Environ. Prot., 116 (2018) 262–286.
[4] T. Ahmad, C. Guria, A. Mandal, A review of oily wastewater treatment using ultrafiltration membrane: a parametric study to enhance the membrane performance, J. Water Process Eng., 36 (2020) 101289, doi: 10.1016/j.jwpe.2020.101289.
[5] S. Sabir, Approach of cost-effective adsorbents for oil removal from oily water, Crit. Rev. Env. Sci. Technol., 45 (2015) 1916–1945.
[6] F.A. Hussain, J. Zamora, I.M. Ferrer, M. Kinyua, J.M. Velázquez, Adsorption of crude oil from crude oil–water emulsion by mesoporous hafnium oxide ceramics, Environ. Sci. Water Res. Technol., 6 (2020) 2035–2042.
[7] S. Putatunda, S. Bhattacharya, D. Sen, C. Bhattacharjee, A review on the application of different treatment processes for emulsified oily wastewater, Int. J. Environ. Sci. Technol., 16 (2019) 2525–2536.
[8] L. Yu, M. Han, F. He, A review of treating oily wastewater, Arabian J. Chem., 10 (2017) S1913–S1922.
[9] K. Abuhasel, M. Kchaou, M. Alquraish, Y. Munusamy, Y.T. Jeng, Oilywastewater treatment: overview of conventional and modern methods, challenges, and future opportunities, Water, 13 (20121) 980, doi: 10.3390/w13070980.
[10] J. Liu, X. Wang, A new method to prepare oil adsorbent utilizing waste paper and its application for oil spill clean-ups, BioResources, 14 (2019) 3886–3898.
[11] Z. Zhang, H. Jin, C. Wu, J. Ji, Efficient production of high-quality few-layer graphene using a simple hydrodynamic-assisted exfoliation method, Nanoscale Res. Lett., 13 (2018) 416, doi: 10.1186/s11671-018-2830-9.
[12] J.M. González-Domínguez, V. León, M.I. Lucío, M. Prato, E. Vázquez, Production of ready-to-use few-layer graphene in aqueous suspensions, Nat. Protoc., 13 (2018) 495–506.
[13] L. Zhou, L. Fox, M. Włodek, L. Islas, A. Slastanova, E. Robles, O. Bikondoa, R. Harniman, N. Fox, M. Cattelan, W.H. Briscoe, Surface structure of few layer graphene, Carbon N.Y., 136 (2018) 255–261.
[14] S. Mitra, S. Banerjee, A. Datta, D. Chakravorty, A brief review on graphene/inorganic nanostructure composites: materials for the future, Indian J. Phys., 90 (2016) 1019–1032.
[15] E. Mohammadi Maroufi, L. Amirkhani, H. Zakaryazadeh, Removal of real multicomponent textile wastewater by adsorption onto graphene oxide nanoparticles: optimization of operating parameters, Desal. Water Treat., 226 (2021) 104–112.
[16] D.M. Mahmudunnabi, M.Z. Alam, M. Nurnabi, Removal of TURQUOISE GN from aqueous solution using graphene oxide, Desal. Water Treat., 174 (2020) 389–399.
[17] K. Takeuchi, H. Kitazawa, M. Fujishige, N. Akuzawa, J. Ortiz-Medina, A. Morelos-Gomez, R. Cruz-Silva, T. Araki, T. Hayashi, M. Endo, Oil removing properties of exfoliated graphite in actual produced water treatment, J. Water Process Eng., 20 (2017) 226–231.
[18] Z. Bano, S.A. Mazari, R.M. Yousaf Saeed, M.A. Majeed, M. Xia, A.Q. Memon, R. Abro, F. Wang, Water decontamination by 3D graphene based materials: a review, J. Water Process Eng., 36 (2020) 101404, doi: 10.1016/j.jwpe.2020.101404.
[19] Mu. Naushad, A New Generation Material Graphene: Applications in Water Technology, Springer Publication, King Saud University, 2019.
[20] S. Gayathri, P. Jayabal, M. Kottaisamy, V. Ramakrishnan, Synthesis of few layer graphene by direct exfoliation of graphite and a Raman spectroscopic study, AIP Adv., 4 (2014) 027116, doi: 10.1063/1.4866595.
[21] T.A. Tabish, F.A. Memon, D.E. Gomez, D.W. Horsell, S. Zhang, A facile synthesis of porous graphene for efficient water and wastewater treatment, Sci. Rep., 8 (2018) 1817, doi: 10.1038/s41598-018-19978-8.
[22] E.-C. Cho, Y.-S. Hsiao, K.-C. Lee, J.-H. Huang, Few-layer graphene based sponge as a highly efficient, recyclable and selective sorbent for organic solvents and oils, RSC Adv., 5 (2015) 53741–53748, doi: 10.1039/C5RA06737E.
[23] A.C. Ferrari, J.C. Meyer, V. Scardaci, C. Casiraghi, M. Lazzeri, F. Mauri, S. Piscanec, D. Jiang, K.S. Novoselov, S. Roth, A.K. Geim, Raman spectrum of graphene and graphene layers, Phys. Rev. Lett., 97 (2006) 187401, doi: 10.1103/PhysRevLett.97.187401.
[24] F. Kwofie, B.K. Lavine, J. Ottaway, K. Booksh, Differentiation of edible oils by type using raman spectroscopy and pattern recognition methods, Appl. Spectrosc., 74 (2020) 645–654.
[25] H. Motahari, R. Malekfar, Laser micro-Raman Spectroscopy of CVD nanocrystalline diamond thin film, Int. J. Opt. Photonics, 13 (2019) 3–12, doi: 10.29252/ijop.13.1.3.
[26] M.A. Saiful Badri, M.M. Salleh, N.F. Md Noor, M.Y.A. Rahman, A.A. Umar, Green synthesis of few-layered graphene from aqueous processed graphite exfoliation for graphene thin film preparation, Mater. Chem. Phys., 193 (2017) 212–219.
[27] Y.F. Hao, Y.Y. Wang, L. Wang, Z.H. Ni, Z.Q. Wang, R. Wang, C.K. Koo, Z.X. Shen, J.T.L. Thong, Probing layer number and stacking order of few-layer graphene by Raman spectroscopy, Small, 6 (2010) 195–200.
[28] X. Wang, L. Zhang, Green and facile production of high-quality graphene from graphite by the combination of hydroxyl radicals and electrical exfoliation in different electrolyte systems, RSC Adv., 9 (2019) 3693–3703.
[29] T. Virtanen, G. Rudolph, A. Lopatina, B. Al-Rudainy, H. Schagerlöf, L. Puro, M. Kallioinen, F. Lipnizki, Analysis of membrane fouling by Brunauer–Emmet–Teller nitrogen adsorption/desorption technique, Sci. Rep., 10 (2020) 3427, doi: 10.1038/s41598-020-59994-1.
[30] F.T. Thema, M.J. Moloto, E.D. Dikio, N.N. Nyangiwe, L. Kotsedi, M. Maaza, M. Khenfouch, Synthesis and characterization of graphene thin films by chemical reduction of exfoliated and intercalated graphite oxide, J. Chem., 2013 (2013) 150536, doi: 10.1155/2013/150536.
[31] T. Holland, A.M. Abdul-Munaim, C. Mandrell, R. Karunanithy, D.G. Watson, P. Sivakumar, UV-Visible spectrophotometer for distinguishing oxidation time of engine oil, Lubricants, 9 (2021) 37, doi: 10.3390/lubricants9040037.
[32] I.N. Evdokimov, A.P. Losev, Potential of UV-visible absorption spectroscopy for characterizing crude petroleum oils, Oil Gas Bus., 1 (2007) 1–21.
[33] D. Boskou, Olive Oil, World Rev. Nutr. Dietetics, 97 (2007) 180–210.
[34] M.A. Al-Ghouti, L. Al-Atoum, Virgin and recycled engine oil differentiation: a spectroscopic study, J. Environ. Manage., 90 (2009) 187–195.